Toxicology in Vitro 29 (2015) 1201–1214

Contents lists available at ScienceDirect

Toxicology in Vitro

journal homepage: www.elsevier.com/locate/toxinvit

Commercial single-walled carbon nanotubes effects in fibrinolysis of human umbilical vein endothelial cells

Yury Rodríguez-Yáñez [a], Daniel Bahena-Uribe [b], Bibiana Chávez-Munguía [c], Rebeca López-Marure [d], Stuart González-Monroy [e], Bulmaro Cisneros [f], Arnulfo Albores [a,*]

[a] Departamento de Toxicología, Centro de Investigación y de Estudios Avanzados del IPN (Cinvestav), Mexico
[b] Laboratorio Avanzado de Nanoscopía Electrónica (LANE), Cinvestav, Mexico
[c] Departamento de Infectómica y Patogénesis Molecular, Cinvestav, Mexico
[d] Departamento de Biología Celular, Instituto Nacional de Cardiología "Ignacio Chávez", Mexico
[e] Hospital General de Ticomán, Secretaría de Salud del Distrito Federal, Mexico
[f] Departamento de Genética y de Biología Molecular, Cinvestav, Mexico

ARTICLE INFO

Article history:
Received 11 December 2014
Accepted 16 February 2015
Available online 16 March 2015

Keywords:
Commercial carbon nanotubes
Endothelial cells
Fibrinolysis
Oxidative stress

ABSTRACT

Recent studies have demonstrated that carbon nanotubes (CNTs) induce platelet aggregation, endothelial dysfunction and vascular thrombosis. However, there is little information on the effects of CNTs on fibrinolysis. We investigated the role of pristine-commercial single-walled carbon nanotubes (SWCNTs) with <3% Co content in fibrinolysis and their contribution to the induction of pro-thrombotic processes in human vein endothelial cells (HUVEC). SWCNTs alone produced concentration-dependent oxidation, as measured by a dithiothreitol oxidation assay. Internalized SWCNTs were located in HUVEC treated with 25 μg/ml using transmission electron microscopy, whereas treatment with 50 μg/ml compromised cell viability, and oxidative stress increased significantly at 5 μg/ml. The study showed that in HUVEC treated with 25 μg SWCNT/ml, fibrinolysis-related gene expression and protein levels had increased by 3–12 h after treatment (*serpine-1*: 13-fold; *PLAT*: 11-fold and *PLAU*: 2-fold), but only the PAI-1 protein was increased (1.5-fold), whereas tissue and urokinase plasminogen activator proteins (tPA and uPA, respectively) tended to decrease. In summary, pristine SWCNTs treatment resulted in evident HUVEC damage caused by cell fiber contact, internalization, and oxidative stress due to contaminant metals. The generation of endothelial dysfunction, as shown by the altered expression of genes and proteins involved in fibrinolysis, suggest that SWCNTs display pro-thrombotic effects.

1. Introduction

At present, nanomaterials have become a valuable raw material used in industry for numerous products with special properties. Carbon nanotubes (CNTs) are a case in point as, since their discovery in 1991 (Iijima, 1991), they have attracted great scientific research and technological attention due to their simple chemical composition, extraordinary properties and versatile applications. However, the human risk of exposure to nanomaterials has not yet been fully characterized (for a review, see Rodriguez-Yanez et al. (2013)). Exposure to CNTs may occur in an occupationally context or derived from the possible use as medical devices. Also, due to the increasing production and use of CNTs, also will increase their release to the environment during their production process. For these reasons, respiratory and vascular system represent a portal of entry of CNTs. Nevertheless, several research groups have studied the biodistribution pathway using different animal models. It is clear that CNT-toxicokinetics depends on the shape, physicochemical properties, impurities and agglomeration of pristine CNTs. These characteristics also determine the CNT-deposition in different regions of the respiratory tract when they are inhaled. To date, there are only a few studies that explain the toxicokinetic

Abbreviations: CNTs, carbon nanotubes; SWCNTs, single-walled carbon nanotubes; MWCNTs, multi-walled carbon nanotubes; HUVEC, human umbilical vein endothelial cells; ECs, endothelial cells; PAs, plasminogen activators; tPA, tissue-plasminogen activator; uPA, urokinase-plasminogen activator; PAI-1, plasminogen activator-1; KKS, kallikrein-kinin system; KLK1, tissue kallikrein; FBS, fetal bovine serum; TNF-α, tumor necrosis factor-alpha; DTT, dithiothreitol; PI, propidium iodide; C-TEM, conventional transmission electron microscope; HR-TEM, high-resolution transmission electron microscope; H_2DCFDA, 2,7-dichlorofluorescein diacetate; ROS, reactive oxygen species; cDNA, complementary DNA; PCR, real-time polymerase chain reaction; ELISA, enzyme-linked immunosorbent assay; FS, fibrinolysis system.

* Corresponding author at: Departamento de Toxicología, Centro de Investigación y de Estudios Avanzados del IPN, Ave. Instituto Politécnico Nacional 2508, Col. San Pedro Zacatenco 07360, P.O. Box: 14-740, México, D.F., Mexico. Tel.: +52 55 57473800x3308; fax: +52 55 57473395.
E-mail address: aalbores@cinvestav.mx (A. Albores).

http://dx.doi.org/10.1016/j.tiv.2015.02.009
0887-2333/

of CNTs, but the most of them have been focused use either as intra-tracheal instillation or intravenous injection, and explain the effects on respiratory and systemic blood circulation. It is possible that after their deposition, CNTs are able to translocate to extrapulmonary sites (Bussy et al., 2013; Ali-Boucetta and Kostarelos, 2013). In this context, Erdely et al. (2013) reported a relationship between pulmonary deposition and systemic circulation, where the CNTs may induce both pulmonary and systemic effects characterized by a blood gene and protein expression pattern. Once CNTs enter the general circulation, they may interact with blood cells, plasma proteins and endothelial cells (ECs).

ECs form a single cell layer called the endothelium, which is localized at the luminal face of the blood vessels and plays a key physiological role in the regulation of fibrinolysis mechanisms through the expression of pro-thrombotic and anti-thrombotic factors in close relationship with smooth muscle cells and the extracellular matrix (Baudin et al., 2007). Human umbilical vein endothelial cells (HUVEC) represent a good model commonly used for physiological, pharmacological and toxicological investigations, such as blood coagulation, macromolecule transport, angiogenesis and fibrinolysis (Bachetti and Morbidelli, 2000) and also for the study of endothelial cell functions due to the fact that they are both anatomically and physiologically representative of arterial blood vessels. Thus, moreover, represents a first approach to the search for mechanisms to explain cellular alterations due to diseases or to the presence of toxic agents.

Fibrinolysis is a complex process with many steps and the participation of numerous molecules, e.g., (a) plasminogen, a pro-enzyme that is converted into plasmin, the active enzyme, depending on the presence of plasminogen activators (PAs), such as tissue-plasminogen activator (tPA) and urokinase-plasminogen activator (uPA), and their inhibitors (PAIs), especially plasminogen activator-1 (PAI-1); (b) the kallikrein-kinin system (KKS), particularly tissue kallikrein (KLK1), which promotes fibrinolysis by stimulating the release of tPA from ECs (Brown et al., 2000; Bhoola et al., 1992).

In vivo, exposure to CNTs results in endothelial dysfunction with neutrophil adhesion to the endothelial monolayer through increases in the expression of adhesion molecules via nuclear NF-κB/P65 translocation, as well as oxidative stress (Zhiqing et al., 2010), the induction of platelet aggregation and an increase in thrombus formation, leading to a decrease in the occlusion time in small mesenteric arteries, which increases vascular thrombosis (Radomski et al., 2005; Bihari et al., 2010). In addition, CNTs affect platelets, which are essential to the coagulation process, promoting their activation *in vitro* leading to their aggregation and viability loss. This process is associated with Ca^{2+} influx and its depletion from intracellular stores (Lacerda et al., 2011; Semberova et al., 2009; Meng et al., 2012), increases in both P-selectin expression and the number of platelet-granulocyte complexes (Bihari et al., 2010), and an up-regulation of glycoprotein integrin receptor GPIIb/IIIa, all of which are crucial for platelet aggregation (Radomski et al., 2005). Additionally, CNTs cause different degrees of red blood cell damage, leading to earlier fibrin formation that might significantly increase the hardness of the clots (Meng et al., 2012).

In spite of the increasing experimental data on the pulmonary effects of CNTs, at present, there are few studies focused on the effects of CNTs on the vascular endothelium, especially toward the coagulation system.

Due to the lack of information about the mechanism by which CNTs may affect fibrinolysis, we investigated the effects of commercial and pristine SWCNTs on primary cultures of human umbilical vein endothelial cells (HUVEC) *in vitro* by assessing the expression of genes/proteins associated with plasminogen activation (*Serpine-1*/PAI-1, *PLAT*/tPA, *PLAU*/uPA), vascular homeostasis (KLK1) and endothelial dysfunction, because ECs might interact with this nanomaterial. In addition, the intrinsic SWCNTs oxidative potential, their cell internalization and their capacity to produced oxidative stress were also studied.

2. Materials and methods

2.1. Carbon nanotubes suspension in culture media

A single-walled carbon nanotubes (SWCNTs) stock was purchased as dry powder from Nanostructured & Amorphous Materials, Inc. (Houston, TX); the physicochemical characterization of SWCNTs is shown in Table 1. The powder sample was dissolved in sterile deionized (DI) H_2O using a biosafety cabinet class III (Esco Technologies, Inc., Singapore, Sin) at a concentration of 4 mg/ml. The stock solution was prepared as previously described (Wang et al., 2010a). The mixture was suspended by sonication at 90 W for 15 min (Branson, Danbury, CT) and used as a stock solution. An appropriate amount of the SWCNT stock solution was added to the culture media to obtain the desired final concentration. The diluted suspensions were vortexed for 15 s, then sonicated for 15 min and vortexed again for 15 s. Here, we used fetal bovine serum (FBS) (Gibco-Life Technologies) as a SWCNT-dispersing agent, and it was added to the culture media before the addition of SWCNTs at a 1% v/v final concentration. Thereafter, we characterized the SWCNT-suspension by assessing its stability index through monitoring the sedimentation kinetics of the suspension's absorbance at 550 nm for different lengths of time in a UV–VIS spectrophotometer (Infinite M200, Tecan Austria GmbH, Austria). An aliquot (1 ml) of the SWCNT-suspension containing 50 μg/ml was prepared with or without FBS, and the absorbance readings were taken at 1 hour-time intervals for 24 h (data not shown).

2.2. Dithiothreitol assay and oxidative activity

The intrinsic redox activity was adapted for SWCNTs from the assay based on the ability of particulate matter components to act as electron transfer agents between dithiothreitol (DTT), as the electron source, and oxygen, as the electron acceptor (Kumagai et al., 2002). The remaining thiol content was allowed to react with DTNB, generating 5-mercapto-2-nitrobenzoic acid, and measured at 412 nm in a spectrophotometer. Briefly, the SWCNT-suspensions (0.01–50 μg corresponding to the following theoretical molarities: 2.94×10^{-15} – 6.32×10^{-16} to 1.47×10^{-11} – 3.16×10^{-12}, as considering the lower and higher SWCNTs dimension limits; http://www.nanointegris.com/en/hipco) were incubated at 37 °C with 0.5 M PBS, pH 7.4, DI H_2O and 1 mM DTT (Sigma–Aldrich) for 0–45 min. Subsequently, 10% trichloroacetic acid (Sigma–Aldrich) was added to an aliquot of the incubation mixture to stop the reaction. Next, an aliquot of the last mixture was dissolved with Tris buffer, pH 8.9, with 20 mM EDTA and 10 mM DTNB (Sigma–Aldrich) solution and

Table 1
Physicochemical characterization of SWCNTs.

Property	Characterization
Purity	95% CNT, 90% SWCNT
Average outside diameter	1–2 nm
Inside diameter	0.8–1.6 nm
Length	1–3 μm
Impurities/contaminants	
Transition metals	Co < 3%
Other elements	Al < 0.1%, Cl < 0.5%, S < 0.3%

Stock#: 1246YJS. Manufacturing method: Catalytic CVD. Analysis Method: Energy Dispersive X-ray Spectroscopy, as reported by the supplier.

was read at 412 nm in a UV–VIS spectrophotometer (Infinite M200, Tecan Austria GmbH, Austria). Redox activity was expressed as the rate of DTT consumption (nmol) per minute per microgram of sample minus the activity observed in the absence of SWCNTs.

2.3. Endothelial primary cell culture

HUVEC were obtained by collagenase digestion by pooling 8–10 umbilical cords per culture plate, obtained from independent donors (all provided by Hospital General de Ticoman-SSDF; Ethical approval by the Hospital Ethics Committee: E1/230/2012). The phenotype of HUVEC cultures was confirmed by VE-cadherin antigen staining and were cultured in M199 medium (Gibco-Life Technologies) supplemented with 10% FBS, 20 μg/ml endothelial mitogen (Sigma–Aldrich) and 1 mg/ml heparin (Pisa pharmaceutical). For the experiments, the HUVEC were always used after the second passage and maintained in DMEM without phenol red (Sigma–Aldrich), with 1% FBS, for 12 h prior to exposure. Subsequently, the HUVEC were exposed to SWCNTs at concentrations of 0.01–25 μg/ml, except for specifically indicated assays, and to tumor necrosis factor-alpha (TNF-α) (Invitrogen-Life Technologies) (10 ng/ml) as a positive control of endothelial activation. Likewise, for some experiments, an antioxidant group was included with the same SWCNTs concentration plus Trolox (Sigma–Aldrich) (50 μg/ml, final concentration).

2.4. Cell viability

Propidium iodide (PI) is a membrane-impermeable dye that is generally excluded from viable cells. It binds to double stranded DNA by intercalating between base pairs. PI is excited at 488 nm and, with a relatively large Stokes shift, emits at a maximum wavelength of 617 nm. Briefly, control and SWCNT-treated HUVEC (1×10^6 cells/100 μl) were placed into FACS tubes and washed two times by adding 2 ml of PBS, centrifuging and the decanting the buffer from the pelleted cells. The cells were re-suspended in 200 μl of staining buffer that contained 10 μg/ml PI (Sigma–Aldrich) in PBS. The mixture was mixed gently and incubated for 1 min in the dark. The PI fluorescence was determined using an FL-2 channel with a flow cytometer (BD FACSCalibur Flow Cytometer; BD Biosciences, San Jose, CA), and at least 10,000 events were used for each measurement.

2.5. Transmission electron microscopy (TEM)

The SWCNT-structure was characterized by TEM. The SWCNT-suspension (5 μg/ml) was deposited in a gold-grid, and the sample was dried and analyzed in a conventional transmission electron microscope (C-TEM) (Jeol JEM 1011, Tokio, Japan) and in a high-resolution transmission electron microscope (HR-TEM) (Jeol JEM-ARM200F, Tokyo, Japan). Images were taken at different magnifications at 80 kV.

On the other hand, cell SWCNT-internalization was observed in treated HUVEC fixed in 2.5% glutaraldehyde in 0.1 M sodium cacodylate buffer for 24 h at 4 °C. The samples were washed with the same buffer and post-fixed with 1% osmium tetroxide containing 0.8% potassium ferrocyanide. The samples were dehydrated with ethanol (70%, 80%, 90% and absolute) and detached with a fast propylene oxide treatment. After incubation in a mixture of propylene oxide-epoxy resin (1:1) for 24 h, the samples were embedded in the epoxy resin POLY/BED 812 (Polysciences, Inc. Warrington, UK) and polymerized for 24 h at 60 °C. Then, 60 nm sections were sieved in 300 mesh cupper-grids and contrasted with uranyl acetate and lead citrate. The sections were examined in a Jeol JEM 1011 and JEM-ARM200F microscopes at 80 kV.

2.6. Index of oxidative stress

This assay is based on the use of dichlorofluorescein diacetate (H_2DCFDA), a cell permeable, non-fluorescent reagent cleaved by intracellular esterases to produce the cell membrane-impermeable, non-fluorescent product H_2DCF, which accumulates intracellularly, where it is oxidized to the highly fluorescent dichlorofluorescein (DCF). The redox state of the sample can be monitored by detecting the increase in fluorescence measured at 530 nm when the sample is excited at 485 nm. Briefly, 1×10^6 cells were incubated in a 6-well plate, and after treatment with SWCNTs (0.01–50 μg/ml) for 2 h, the cells were washed, and the medium was replaced with PBS. H_2DCFDA (Sigma–Aldrich) was dissolved in methanol (10 mM) and added to PBS for a final concentration of 5 μM, and the cells were incubated at 37 °C for 30 min in the dark. The cells were washed with PBS, then trypsinized and washed again with PBS. The mixture was centrifuged, and the supernatant decanted. The cell pellet was re-suspended in 200 μl of PBS, covered and kept away from light. The fluorescence was determined using a FL-1 channel with a flow cytometer (BD FACSCalibur Flow Cytometer; BD Biosciences, San Jose, CA), and at least 10,000 events were used for each measurement.

2.7. RNA isolation

Total RNA was extracted from control and SWCNT-treated cells using TRIzol® reagent (Invitrogen-Life Technologies) according to the manufacturer's instructions. The RNA concentration and purity were estimated by optical density at 260/280 nm, and its integrity was assessed by electrophoresis on 1% agarose gels stained with ethidium bromide. Isolated RNA was stored at −70 °C until analysis.

2.8. Complementary DNA (cDNA) synthesis and real-time polymerase chain reaction (PCR)

cDNA was synthesized using amplification grade DNAse and SuperScript® III First-strand synthesis system (Invitrogen-Life Technologies) according to the manufacturer's instructions. Real-time PCR reactions were carried out in a CFX96 Real-time PCR Detection system (BioRad Laboratories Inc., Hercules, CA) using the TaqMan® Universal PCR Master Mix (Applied Biosystems-Life Technologies). In a final volume of 15 μl, 1 μl of cDNA was amplified using the following Taqman® gene expression assays (Applied Biosystems-Life Technologies): *Serpine-1* (Hs01126606_m1), *PLAT* (Hs00938315_m1), *PLAU* (Hs01547054_m1), *KLK1* (Hs00158490_m1) and *GAPDH* (Hs02758991). The relative mRNA levels were calculated according to the comparative C_t method, using *GAPDH* as a housekeeping gene.

2.9. PAI-1, tPA, and uPA quantitation

Cell culture supernatants of both control and SWCNT-treated cells were used after a specified time of exposure. Briefly, the PAI-1, tPA and uPA were assessed using commercially available enzyme-linked immunosorbent assay (ELISA) kits (Abcam) and according to the suppliers indications. Polyclonal antibodies specific for each antigen were pre-coated onto a microplate. The antigen in standards and samples (cell culture supernatants) was sandwiched by the immobilized antibody and a biotinylated polyclonal antibody specific for each antigen, which was recognized by streptavidin-peroxidase conjugating agent. All unbound material was then washed away, and a peroxidase enzyme substrate was added. Color development was stopped as indicated, and its intensity was measured in a microplate reader (Infinite M200, Tecan Austria GmbH, Austria).

2.10. Statistical analysis

The results shown are the mean values ± the standard error of the mean (SEM) of three independent experiments performed in triplicate. Data were analyzed using one-way analysis of variance (ANOVA), followed by Dunnet's *post hoc* test. qPCR data were analyzed using the Kruskal–Wallis/one-way ANOVA, followed by Dunn's *post hoc* test.

All statistical analyses were performed by Graphpad Prism software version 6.0 (Graphpad Software Inc. San Diego, CA). Differences were considered statistically significant at $^{*}p < 0.05$ or $^{**}p < 0.01$.

3. Results

3.1. SWCNT characterization

Physicochemical characteristics and TEM micrograph of the SWCNTs used in this study are shown in Table 1 and Fig. 1, respectively. The external diameter of a CNT was 1–2 nm, which is in accordance with the definition of nanomaterial. Ninety-five percent of the material supplied were CNTs and of these, ninety percent were SWCNTs. Co was the main impurity (<3%), and other elements were present at low concentrations. The CNTs contained metals that were used in their fabrication and were difficult to remove; these metals are considered impurities or contaminants and should be considered when interpreting the results. The metal content in the CNTs used in other investigations is shown in Table 2, with Co concentrations ranking from 0.4% to 5% of the raw material weigh; however, some other elements could be present at even higher concentrations. Thus, each study of CNTs can be considered independent, with findings reflecting only their particular composition.

3.2. Intrinsic REDOX activity of SWCNTs

An assessment of the oxidative ability of pristine SWCNTs was conducted using a DTT assay. The results show that SWCNTs had a high DTT oxidative capacity in a concentration-dependent manner, which was significant at 5 μg/ml and above (Fig. 2). SWCNTs contain some elements used in their fabrication; in this case, the content of Co, a transition metal, was <3%, and that of other elements was <1%. Thus, the DTT assay indicated the possible oxidation capacity of both SWCNTs and their contaminating metals. This oxidative capacity may promote oxidative cell damage.

Table 2
Contaminants reported on CNT material used *in vitro* and *in vivo* studies.

Metal	% Material	CNT concentration	References
Fe	30	0.06–0.24 mg/l	Shvedova et al. (2003)
	0.23	0–40 μg/mouse	Shvedova et al. (2005)
	0.23	0–96 μg/cm^2	Kisin et al. (2007)
	17.7	5–20 μg/mouse	Shvedova et al. (2008)
	10	0.01–1 mg/l	Guo et al. (2008)
	0.07	5 and 50 μg/cm^2	Pacurari et al. (2008)
	Raw: 30; Purified: 0.23	75 mg/ml; 60–240 μg/ml	Murray et al. (2009)
	0.32	10–80 μg/mouse	Porter et al. (2010)
Fe, Ni, Cu	Raw: 26.9, 0.78, 0.36 Purified: 2.14	0.1–0.5 mg/mouse	Lam et al. (2004)
Fe, Co	<1.3, <0.4	7.5–30 μg/ml	Wick et al. (2007)
Fe, Ni, Y	10, 3, 2	0–0.8 mg/ml	Casey et al. (2008)
	10, <1, <1	0–400 μg/ml	Herzog et al. (2007)
Co, Ni	2.5	50 μg/ml	Worle-Knirsch et al. (2006)
	5	0–50 mg/kg	Warheit (2009)
Co	<3	0.01–50 μg/ml	This study

3.3. SWCNT cytotoxicity on HUVEC

HUVEC were exposed to pristine SWCNTs (5–500 μg/ml) for 24 h to assess cell viability with the PI method. Increasing concentrations of SWCNTs resulted in a decrease in HUVEC viability that reached statistical significance at 50 μg SWCNTs/ml and above compared with untreated control cell cultures. At 50 μg SWCNTs/ml, cell viability decreased approximately 20%, and the decrease was even higher when exposed to 100 μg/ml (Fig. 3). Based on these results, all of our subsequent experiments with HUVEC were performed using concentrations ranging from 0.01 to 50 μg SWCNTs/ml.

3.4. Cellular redox state

It is well known that H_2DCFDA cannot be used as direct measure of ROS due to it reacts with several one-electron oxidizing species (e.g. hydroxyl radicals) or redox-active metals

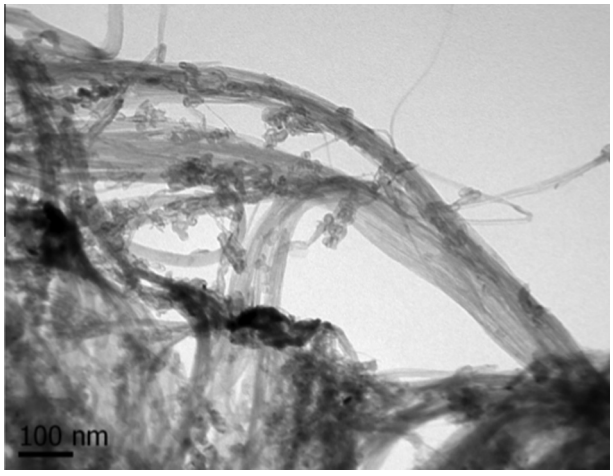

Fig. 1. Representative micrograph of SWCNTs. TEM images of SWCNTs (Jeol JEM 1011 operated at 80 kV).

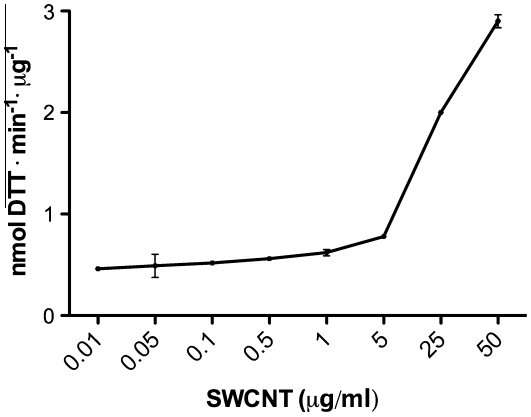

Fig. 2. REDOX activity of SWCNTs assessed by dithiothreitol assay. Activity is expressed as the rate of DTT consumption after a 15 min of incubation (nmol DTT min^{-1} μg^{-1}) of sample minus the activity obtained in absence of SWCNTs. Data are present as mean ± SEM of three independent experiments each one by triplicate for each condition.

(Kalyanaraman et al., 2012). For this reason, H_2DCFDA may be used as redox indicator. HUVECs treated with pristine SWCNTs (0.01–50 μg/ml) for 2 h showed a statistically significant increase in oxidative stress that peaked at 5 μg/ml, then decreased at higher concentrations (Fig. 4), where cell viability was clearly affected at 50 μg/ml SWCNT.

3.5. SWCNT-internalization into endothelial cells

The uptake of SWCNTs by HUVEC was visualized by TEM. HUVECs were exposed to 5 or 25 μg/ml SWCNTs for 24 h, then, HUVECs were collected and observed under TEM. The micrographs show that once inside the cell, SWCNTs tend to aggregate and form bundles that look like electron-dense particles mainly in the cytosol and into endocytic vesicles (Fig. 5). At 25 μg/ml, SWCNTs caused vacuole enlargement and the disorganization of mitochondria (Panel B) and accumulated in the cytosol, forming aggregates (Panel C). A control cell is shown in Panel A.

HUVEC-treated (25 μg/ml) preparations were observed under High-Angle Annular Dark Field (HAADF) Scanning Transmission Electron Microscopy (STEM) and Bright Field (BF)-STEM (Fig. 6). Micrographs were taken at different magnifications and showed the presence of SWCNTs in the cytosol near the cell membrane (Panels A–C), which was confirmed by high resolution (Panels D and E).

3.6. SWCNT effects on fibrinolysis genes and anti-oxidant prevention

The effect of SWCNTs (5 or 25 μg/ml) on the *Serpine-1*, *PLAT*, *PLAU* and *KLK1* expression was investigated in HUVEC. TNF-α was used as a positive control for endothelial activation, and Trolox (50 μg/ml) was used as an antioxidant. The expression of the four genes investigated increased between 6 and 12 h after the addition of SWCNTs to HUVEC, and the intensity and duration of the response was specific for each gene.

Treatment with SWCNTs increased the expression of fibrinolysis genes. (1) *Serpine-1* increased 5- and 3.2-fold between 6 and 12 h after treatment with 5 μg/ml, respectively, and 3- to 14.5-fold when treated with 25 μg/ml at the same time points, then decreased to 0.7-fold compared to control values by 24 h. When Trolox was added to the treated HUVEC, the SWCNT effects were prevented. TNF-α increased *Serpine-1* expression 4-fold by 24 h (Fig. 7A). (2) *PLAT* expression increased 4- to 10-fold by 3 and 6 h after SWCNT treatment (5 μg/ml) to HUVEC, respectively.

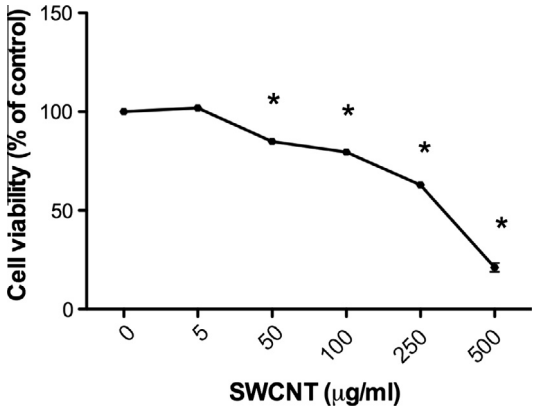

Fig. 3. Effect of 24 h exposure to SWCNTs on HUVEC viability using propidium iodide staining. Fluorescence values were normalized to control values. Data are present as mean ± SEM of three independent experiments each one by triplicate for each condition. *Statistically significant compared to untreated control at $p < 0.05$ by one-way ANOVA/Dunnet's post-test.

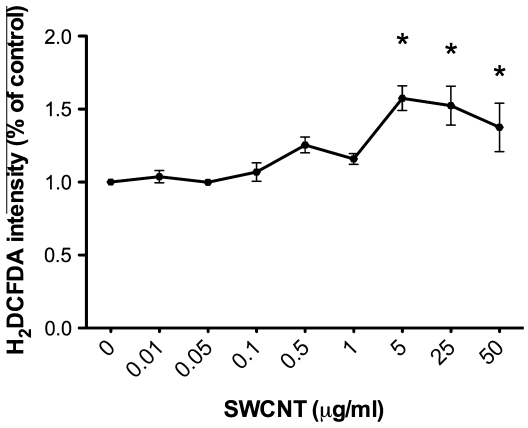

Fig. 4. Effect of SWCNTs on the cellular REDOX state. The cellular REDOX state was measured by the detection of H_2DCFDA fluorescent signal continuously for 2 h in HUVECs by flow cytometry. The graph shows the increase in the percent of oxidative stress at the different concentration of SWCNTs compared to untreated control. Data are present as mean ± SEM of three independent experiments each one by triplicate for each condition. *Statistically significant compared to untreated control at $p < 0.05$ by one-way ANOVA/Dunnet's post-test.

Treatment with higher concentrations of SWCNTs resulted in 7-fold increases by 12 h after treatment and was almost negligible by 24 h at any of the treatments assayed. The addition of Trolox to HUVECs treated with SWCNTs (5 μg/ml) prevented the increases in *PLAT* expression, except at 6 h, when a 2.5-fold increase was observed. The addition of TNF-α to HUVECs increased *PLAT* expression 13-fold at 6 h after SWCNT treatment, then decreased it to 2-fold by 12 h, and the effect was almost negligible by 24 h (Fig. 7B). (3) In contrast, SWCNTs (5 μg/ml) added to HUVEC resulted in a modest 1.5- to 1.8-fold increase in *PLAU* expression by 3 and 12 h, respectively, whereas HUVEC exposed to 25 μg SWCNT/ml increased *PLAU* expression 3.3-fold by 12 h only, with a return to control values by 24 h. Trolox prevented any effect on *PLAU* expression in all SWCNT-treated HUVEC. The addition of TNF-α to HUVEC did not significantly increase *PLAU* expression (Fig. 7C). (4) Finally, *KLK1* expression was increased 4.8- and 1.8-fold at 6 and 12 h after 5 μg/ml addition to HUVEC, respectively. When treated with 25 μg/ml, the increases were 2.6-fold and twice at 6 and 12 h, respectively. By 24 h, the expression levels were similar to control values. Trolox was co-administered with SWCNTs (5 μg/ml) and observed 12 h afterward. *KLK1* expression increased approximately 1.2-fold. TNF-α decreased *KLK1* expression 0.5-fold at the 3 h time point; then, expression increased 2.2-, 5.6- and 18-fold at 6, 12 and 24 h after treatment, respectively (Fig. 7D).

3.7. SWCNT-effects on fibrinolysis proteins and anti-oxidant effects

The effect of SWCNTs (5 or 25 μg/ml) on PAI-1, tPA and uPA levels was investigated in HUVEC. Trolox (50 μg/ml) was used as an anti-oxidant, and TNF-α was used as a positive control for endothelial activation.

The SWCNT treatment had several effects on the fibrinolysis proteins. (1) SWCNT (5 and 25 μg/ml) increased PAI-1 content 1.5-fold. The addition of Trolox (50 μg/ml) to SWCNT-treated HUVEC caused different responses: at 5 μg/ml, a 2.4-fold increase was observed; in contrast, 25 μg/ml caused a 0.4-fold decrease. TNF-α caused a slight, but statistically significant PAI-1 increase (Fig. 8A). (2) tPA levels in HUVEC exposed to SWCNTs (5 and 25 μg/ml) were decreased 0.4-fold. The addition of Trolox decreased tPA 0.65-fold, and TNF-α decreased t-PA 0.8-fold (Fig. 8B). (3) Finally, in HUVEC exposed to SWCNTs (5 μg/ml), uPA levels increased 1.5-fold, whereas 25 μg/ml caused no change.

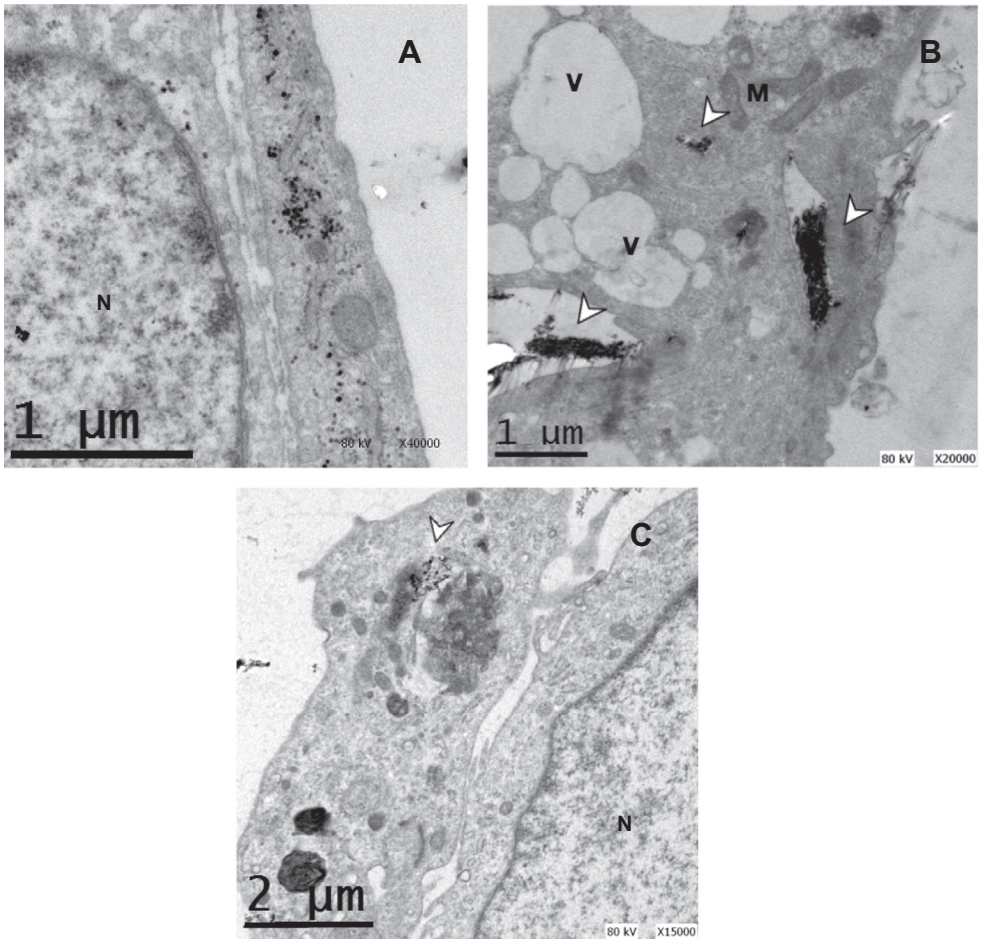

Fig. 5. Internalization of SWCNTs by endothelial cells in HUVEC. TEM of human vein endothelial cells at 24 h after SWCNTs exposure showing nanotubes internalization into endothelial cells. (A) untreated-control, (B, C) 25 µg/ml. Arrows indicate the presence of CNTs into the cell. M, N, V stands for mitochondria, nucleus and vacuoles, respectively.

The addition of Trolox to 5 µg/ml caused a 0.4-fold decrease. TNF-α caused no change (Fig. 8C).

4. Discussion

SWCNTs are promising nanomaterials with increasing industrial demand and diversifying applications but with unknown risks related to human environmental and occupational exposures. Therefore, we studied the capacity of pristine SWCNTs to change the cellular redox state and their effects on cell morphology, specifically, on the fibrinolysis system in a HUVEC culture. The pristine SWCNTs physicochemical characteristics and oxidant properties are also reported.

The synthesis of CNTs consists in producing carbon fragments that are reconstituted to form tubes in the presence of metallic catalyst such as Fe, Co, Ni, among other transition metals at high temperatures (Popov, 2004). Thus, all CNTs produced contain residual amounts of metals which may be removed, but no purification process is totally efficient. By this reason, even purified CNTs samples are not completely metal free and also their toxicity will depend on the redox transition metal used as catalyzer, which will further participate in oxidative stress process. The oxidative capacity of these commercial and pristine SWCNTs can be attributed to the SWCNTs themselves, metal catalytic residues and amorphous carbon. The material used here contained Co (<3%), a transition metal used as a catalyzer in the fabrication of SWCNTs, that remains in the nanotube as a contaminant metal either adsorbed on the surface of the graphene layer or bound into the graphene net (Banhart, 2009). The synthesis of CNTs requires nanometer-size metal particles to act as catalyzers (especially transition metals, due to their electronic structure), where the bonding between metal and carbon increases with the number of unfilled *d*-orbitals; also, Ni, Fe and Co, with similar characteristics, have high affinity to and solubility in the carbon matrix. Conversely, Au or Pd, which have no unfilled *d*-orbitals, are not useful for CNT-synthesis. Additionally, metal atoms interact with the graphene layer by adsorption on the surface or by substitution of one or several carbon atoms, where some metals prefer positions above the center of a hexagon, whereas others prefer positions above a C atom or bridge sites over the edge of the hexagon; either way, the metal will retain its redox properties (Ding et al., 2008; Banhart, 2009). A comparison between the impurities reported by the pristine SWCNTs supplied and those used in other studies is shown in Table 2. The SWCNTs used here had characteristics similar to those used in other studies.

The sharp increase in DTT oxidation by pristine SWCNTs (from 5 µg/ml) could be attributed to the presence of Co (<3%, approximately 0.15 µg Co/ml), the only transition metal reported by the supplier. This response is consistent with the DTT loss and ROS production linked to the metal content in particulate matter (PM) that ranges from approximately 0.9% to 52.8% (Wang et al., 2010b; Vidrio et al., 2009; Shen and Anastasio, 2012; Ntziachristos et al., 2007; Hu et al., 2008; Geller et al., 2006;

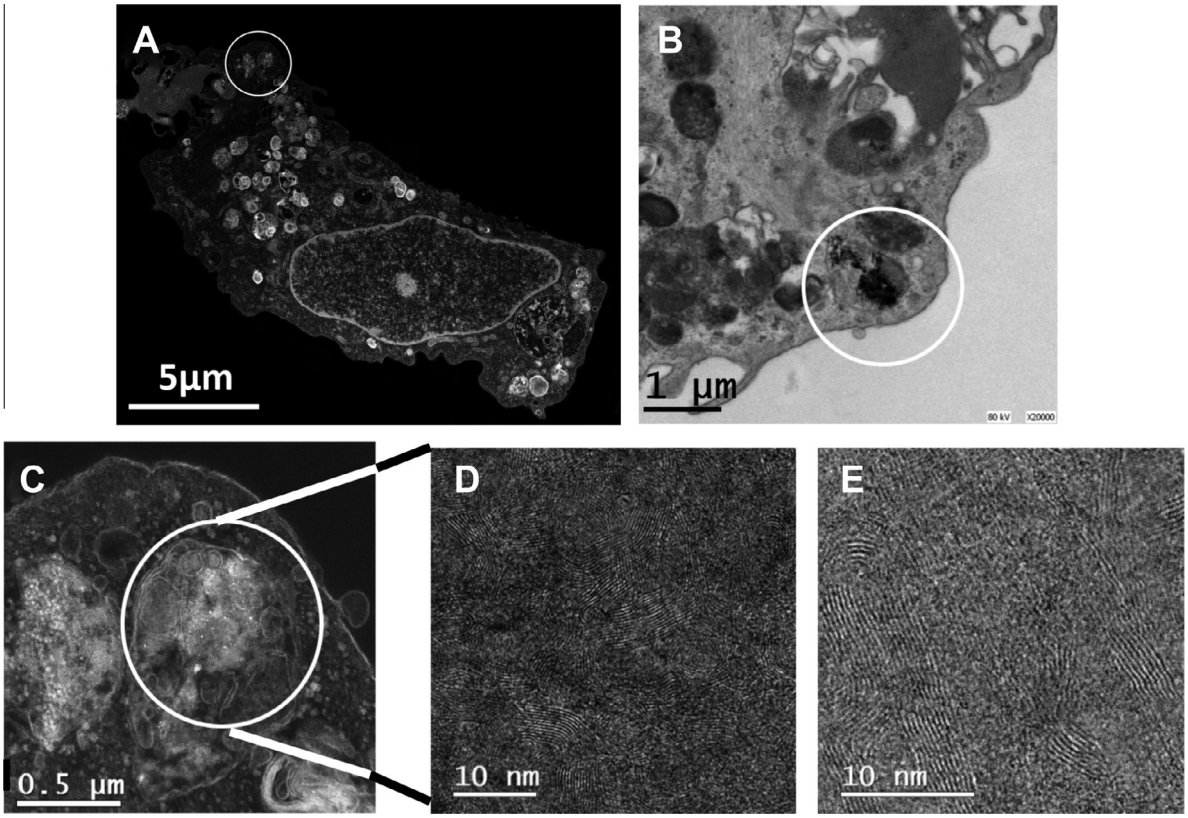

Fig. 6. Scanning transmission electron microscopy imaging of SWCNTs internalization by HUVEC. (A, C) HAADF-STEM images of the cell where the selected areas with CNT-internalized are indicated with a white circle. (B) TEM image of selected area (white circle of figure A) with the CNT-internalized; (D, E) BF-STEM images of CNT into the cell. The images show the previous selected areas in white circles indicated in A–C micrographs; imaging with Atomic Resolution Analytical Electron Microscope JEM ARM200F (JEOL), operated at 80 kV in STEM mode.

DiStefano et al., 2009; Charrier and Anastasio, 2012). Other DTT oxidizing agents reported in PM are carbonaceous compounds, such as polycyclic aromatic hydrocarbons (Li et al., 2003).

Internalization is the first event in the toxic process for pristine SWCNTs and was observed at concentrations starting from 25 µg/ml onwards, which was similar to results that were previously reported for different cell types (Zhu et al., 2007; Simon-Deckers et al., 2008; Sato et al., 2005; Pulskamp et al., 2007; Monteiro-Riviere et al., 2005; Marangon et al., 2012; Foldbjerg et al., 2014). CNTs were visualized as aggregates inside the cell, either dispersed in the cytosol or included into lysosomes (Fig. 5). Despite many efforts, however, the exact mechanism for the internalization of CNTs is unclear, but it could be speculated that the process is dependent on the SWCNT-aggregation status and fiber-like shape and also on the cell type. Although we cannot offer an internalization mechanism, several paths can be proposed (Rodriguez-Yanez et al., 2013; Firme and Bandaru, 2010). Taking into account that CNTs are flexible, lipid-soluble, hydrophobic, tubular structures with a diameter between 0.4 and 4 nm, which are smaller than the pores present in the nuclear membrane, and that they have a comparable size to other pores that serve as ion channels in the plasma membrane (Kostarelos et al., 2007), we hypothesized that in this study, the mechanism of internalization may be carried out by both endocytosis (due to the presence of aggregates in vesicles) and nanopenetration/diffusion (Rodriguez-Yanez et al., 2013; Firme and Bandaru, 2010).

SWCNTs decreased HUVEC viability in a concentration-dependent manner as 50 µg/ml decreased viability to approximately 20% compared to the untreated controls. At that concentration both the formation of aggregates 24 h after exposure and the release of metal impurities contributed to this effect. The SWCNT-concentrations used in this work were chosen from previous studies that demonstrated *in vitro* alterations at the vascular/endothelial levels (Walker et al., 2009; Cheng et al., 2011; Albini et al., 2010). The SWCNT-effects observed here can be produced by other nanomaterials that are able to cause damage to endothelial cells with concentrations similar to those used in this work (Table 3). Although NIOSH recommends an exposure limit of 1 µg/m^3 based on CNT-animal studies (NIOSH, 2013), environmental monitoring on CNTs in the workplace report significant variable concentrations that must also be considered (Table 4). Thus, the concentration range used in this work is environmentally relevant, if the CNT-levels measured in different workplaces are taken into account. Also relevant is the Co content in SWCNTs because Co alone decreases cell viability (Table 5).

The fiber-like shape of SWCNTs promotes morphological changes in HUVEC through cell membrane damage. Due to their shape, the CNT-cell interactions alter cell membrane integrity and/or cellular biochemical processes and interact with matrix adhesion proteins that cause membrane changes and/or the displacement of organelles (Tian et al., 2006) (Porter et al., 2007; Kostarelos et al., 2007). Additionally, SWCNTs cause mitotic disruption because of their physical similarity (size, shape and aggregation) to the microtubules that form the spindle apparatus (Sargent et al., 2009). In addition, SWCNTs alter actin structures, leading to a reduction in cell proliferation (Holt et al., 2010). Thus, the SWCNT-induced damage to the cells studied in this paper could be attributed to both the nanotubes themselves and the presence of Co.

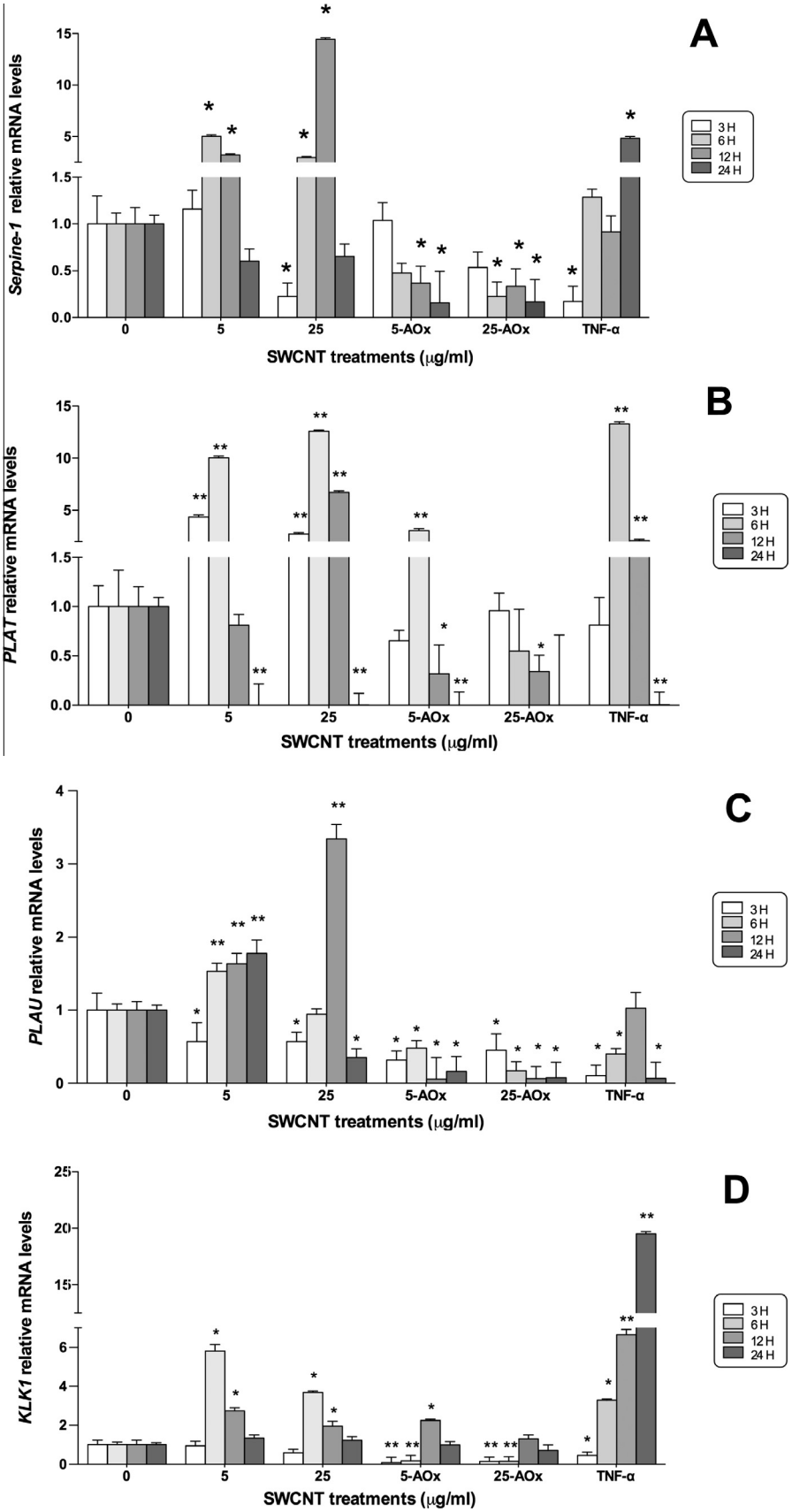

Fig. 7. SWCNTs effect with or without Trolox on the relative expression of *Serpine-1*-, *PLAT*-, *PLAU*- and *KLK1*-mRNA in HUVEC. Total mRNA was isolated from HUVEC confluent cultures untreated and exposed to 5 or 25 μg SWCNT/ml plus antioxidant treatment (AOx) in FBS-1% DMEM. (A) *Serpine-1*-, (B) *tPA*-, (C) *uPA*-, and (D) *KLK1*-mRNA were measured by real-time RT-PCR at 3, 6, 12 or 24 h of exposure. Data are present as mean ± SEM of three independent experiments each one by triplicate for each condition. $^{*}p < 0.05$ and $^{**}p < 0.01$ compared to untreated control by Kruskal–Wallis one-way ANOVA/Dunn's post test.

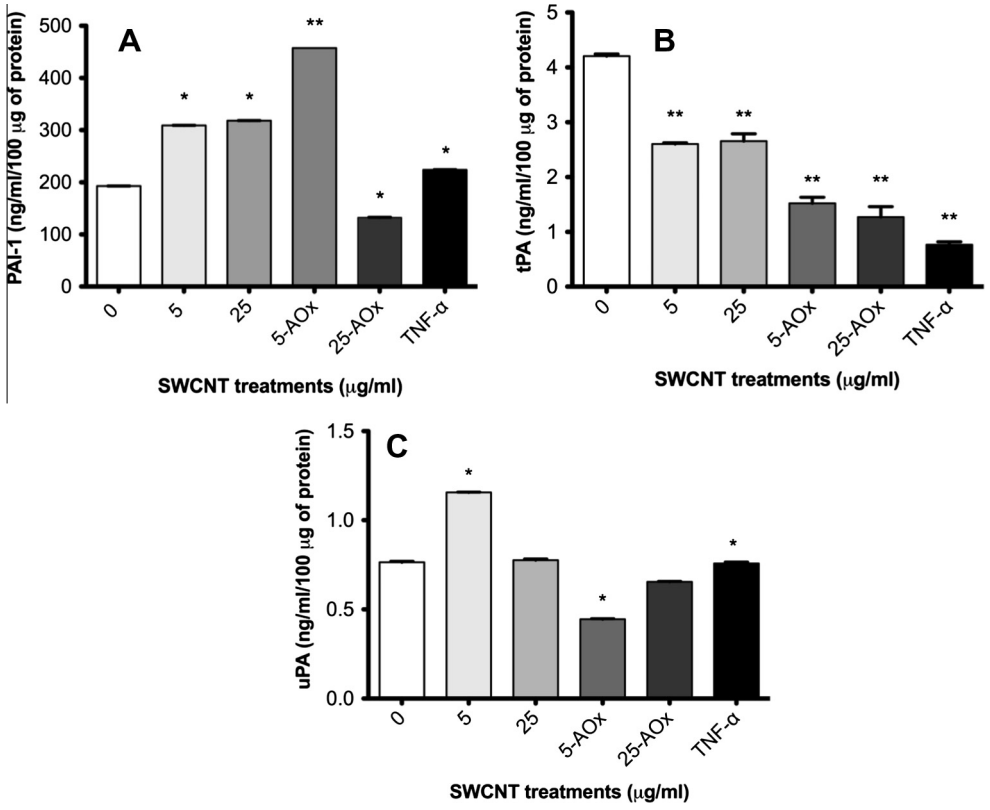

Fig. 8. SWCNTs effect with or without Trolox on Fibrinolysis-protein levels in HUVEC. The cell culture supernatants both of control and SWCNTs (5 or 25 μg/ml)-treated cells, plus antioxidant treatment (AOx) 12 h after exposure. (A) PAI-1, (B) tPA and (C) uPA levels were detected by commercially available ELISA kits and according to the manufacturer instructions. Data are present as mean ± SEM of three independent experiments each one by triplicate for each condition. $^{*}p < 0.05$ and $^{**}p < 0.01$ compared to untreated control by one-way ANOVA/Dunnet's post-test.

The physical structure of SWCNT and the Co contamination content caused an increase in the oxidative stress at 5 μg/ml and above and peaked at 25 μg/ml. Changes in redox state could be related to a direct effect of the SWCNTs on the inner membrane of mitochondria, causing a depolarization that is attenuated by antioxidants (He et al., 2012). In addition to this, the Co contamination present in the SWCNTs may undergo redox cycles, generating $OH^{\cdot}$ and other reactive oxygen species through Fenton reactions (Leonard et al., 1998; Jomova and Valko, 2011). Additionally, ROS formation is associated with metals bound to graphene layers, but also to metals leached from CNTs that reduce antioxidant levels (Ge et al., 2012). Therefore, we demonstrated that the oxidative stress increased as the concentration of SWCNTs increased in exposed HUVEC. This increase may stimulate antioxidant activities in the cell, such as GSH increases; however, when ROS production overwhelms the compensation limit, an irreversible damage is produced (Guo et al., 2011). Finally, concentrations higher than 50 μg/ml slightly decreased the oxidative stress, most likely because cell viability is compromised not only by ROS, but also by the physical interference of CNTs with cellular components.

Because SWCNTs have proved to be able to interact either directly or through the leached metals adsorbed or integrated into the graphene matrix, it could be expected that they may exert toxicity in the place where they are located; thus, the fibrinolysis system (FS) will be affected in ECs when exposed to CNTs.

TEM showed that SWCNTs are internalized into ECs. For this reason, in humans or *in vivo* systems, SWCNTs could be translocated from airways or the lung into the general circulation; therefore, the vasculature becomes a primary target (Nemmar et al., 2002, 2004). Such translocation is favored by the proximity between lung epithelial type 1 cells and the caveolar membrane of the endothelial cells (Heckel et al., 2004). In addition, there is a direct interaction between CNTs, erythrocytes and other blood elements that may contribute to the risk of suffering thrombotic/atherothrombotic injuries.

On other hand, the FS plays a key role in the dissolution of blood clots and the prevention of intravascular thrombosis; thus, its imbalance is involved in the pathophysiology of cardiovascular ischemia and endothelial dysfunction. In addition, this system is also involved in diverse pathologic conditions, such as the formation and progression of cancer, pathogen virulence, airway disease, metabolic disease, chronic inflammatory diseases and others (Rein-Smith and Church, 2014).

In this study, we demonstrated that the exposure of HUVEC to SWCNTs alters gene expression and protein levels involved in fibrinolysis, such as tPA, uPA, KLK1 and PAI-1, the latter being the major fibrinolysis physiological regulator (Binder et al., 2002).

We show that the expressions of the main genes involved in FS were affected by SWCNT-exposure compared to untreated control cells, as shown by the *Serpine-1*-, *PLAT*-, *PLAU*- and *KLK1*-mRNA increases in the first 12 h. These expressions were diminished to levels even lower than the controls after a 24 h treatment. These results are in agreement with those showed previously (Erdely et al., 2009), where it was demonstrated that SWCNTs and MWCNTs deposited in the lung of treated mice. Such deposition activated acute local and systemic responses characterized by changes in blood genes and protein expressions, which, in turn, induced cardiovascular damage. In this study, the SWCNTs used were 0.8–1.2 nm in diameter and 0.1–1 μm in length, and included 8.8% Fe content, and the concentrations were similar to those used in this study. Although this was an *in vitro* study, it agrees with the

Table 3
Effects produced by different types of nanomaterials on endothelial cells.

Nanomaterial	Concentration	Cell culture	Effects	References
Fe_2O_3-, Y_2O_3-, CeO_2-, ZnO-NP	0.001–50 μg/ml	HAEC	Inflammatory response and ROS production with Ce- and Zn-NP above 10 μg/ml Loss of adherence with ZnO-NP	Gojova et al. (2007)
Fe_2O_3-NP	50 μg/ml	HMVEC	Increased cell permeability and stabilization of microtubules through ROS and AKT/GSK-3β	Apopa et al. (2009)
SWCNT, MWCNT, carbon black (CB)-NP	10–150 μg/10^6 cells	HAEC	Actin filaments, VE cadherin disruption, citotoxicity, reduced tubule formation only with CNTs	Walker et al. (2009)
Fe_2O_3-NP	0.1–100 mM	HUVEC	Concentration-dependent loss of cell viability. Cytoskeleton and related functional alterations. Cell migration/invasion inhibition	Wu et al. (2010)
Pristine-SWCNT COOH-MWCNT	12.5–800 μg/ml	HUVEC-EC-C	Both SWCNT and MWCNT induce toxic effects. CNT functionalization and toxicity	Gutierrez-Praena et al. (2011)
Fe_2O_3-NP Fe_3O_4-NP	2–100 μg/ml	HAEC	Increased surface expression of intracellular ICAM-1 and vascular adhesion molecules-1 (VCAM-1) at 100 μg/ml. Increased ROS production and damage to cell membranes	Zhu et al. (2011)
CB-NP	0–100 μg/ml	HUVEC	Inhibition of proliferation, apoptosis and necrosis (from 5 μg/cm^2). Endothelial activation with increase of adhesion and inflammatory molecules. ROS and NO production. NF-κβ pathway activation	Vesterdal et al. (2012)
TiO_2-NP	5–40 μg/cm^2	HUVEC	Inhibition of proliferation, apoptosis and necrosis (from 5 μg/cm^2). Endothelial activation with increases on adhesion and inflammatory molecules. ROS and NO production. NF-κβ pathway activation	Montiel-Davalos et al. (2012)
MWCNT	1 or 10 μg/ml	HAEC	Increase on mRNA transcripts for VCAM-1, SELEICAM-1, and CCL2 in MWCNT with surfactant	Vidanapathirana et al. (2012)
MWCNT	2.5 μg/ml	HMVEC	Increase on cell permeability, migration and ROS production with actin filament remodeling. Induction of MCP-1 and ICAM-1	Pacurari et al. (2012)
Silica NP (SIO3-310-P) (SIO2-304)	$1 \times 10^3 - 6 \times 10^4$ NP per cell/100 μl	HUVEC HeLA	NP-uptake via clatrin dependent pathway. Decrease of mitochondrial activity. Cell dead for HUVEC	Blechinger et al. (2013)
Silica NP	25–100 μg/ml	HUVEC	ROS production, oxidative damage and malondialdehyde production. Inhibition of SOD and GPX. Necrosis and apoptosis after 24 h. Decrease of mitochondrial membrane potential. DNA damage. G2/M arrest via Chk1-dependent	Duan et al. (2013)
MWCNT	1.32 μg/ml	SAEC/HMVEC	Increase in phospho-NF-κβ/Stat3- and p38 MAPK through ROS. Actin rearrangement. Loss of VE-cadherin. Increase of angiogenic ability, as well as VEGFA, sICAM-1 and sVCAM-1	Snyder-Talkington et al. (2013)
Pristine SWCNT	01–50 μg/ml	HUVEC primary cultures	Citotoxicity, cell damage, ROS increases, fibrinolysis- related gene and proteins alterations	This study

Table 4
CNT mass concentration in working environments.

CNT sample	Place	Concentration measured (μg/m^3)	References
MWCNT	AS	36.6–331.7	Han et al. (2008)
MWCNT	AS PBZ	12.6–187.3 7.8–320.8	Lee et al. (2010)
MWCNT SWCNT	PBZ AS PBZ AS	0.8–7.86 0.47–4.62 0.68–3.28 0.82–1.13	Dahm et al. (2012)
SWCNT	Gloves Personal air sample	0.2–6 × 10^3* 0.7–53	Maynard et al. (2004)
SWCNT	PBZ	38	Methner et al. (2012)
MWCNT SWCNT	AS	10–3468 10–83	Dahm et al. (2013)
MWCNT	PBZ	10.6	Erdely et al. (2013)
MWCNT	AS	<430–6800	Hedmer et al. (2014)

Abbreviations: AS (area sample); PBZ (personal breathing zone).
* μg per hand.

one above and reflects the fact that SWCNTs are able to alter the fibrinolysis pathway. Likewise, all mRNA studied were similarly affected by SWCNT-exposure because they all share *cis*-regulatory elements in their promoter, such as CCAAT box-binding transcription factor (CTF)/nuclear factor 1 (NF1), upstream stimulatory factors 1 and 2 (USF1/2), Smad2 and Smad3, CREB-binding protein (CBP) and specificity protein 1 (Sp1), as well as numerous transcription factors, including C/EBP, AP-1, C-FOS, C-JUN, NF-κB, SREBP, CREB, PPARγ, STAT. Additionally, it is important to note that some factors in the mitogen-activated protein kinase (MAPK) pathway are redox-sensitive (see reviews:(Nagamine, 2008; Irigoyen et al., 1999)). In this work, co-treatment with the antioxidant Trolox decreased the mRNA expression levels in HUVEC-treated cells. Additionally, TNF-α, a positive endothelial dysfunction control, increased the mRNA expression, but in a smaller proportion than the SWCNT-exposure concentrations used here. This fact may explain the possible participation of ROS produced by SWCNT-exposure because they are involved in the activation of AP-1 and NF-κB. AP-1 is one of the transcription factors involved in the oxidative stress response after changes in the cellular oxidative status. In this respect, AP-1 has been identified as a target of the MAPK family, which includes ERKs, JNKs, and p38 kinase (Karin et al., 1997). In addition, the activation of NF-κB has been shown to be regulated by some upstream MAPKs that regulate JNK activation in the cells (Ding et al., 2001). Hence, it was previously demonstrated that SWCNT exposure in human lung fibroblasts induces ROS generation and activates PARP, AP-1, NF-κB, p38, and AKT in a dose-dependent manner (Azad et al., 2013). Therefore, some of these pathways may be activated by

Table 5
Co concentrations and its effect on cell viability.

Sample	Cell line	Metal or residue	% WT	Sample and metal concentration	Effect (after 24 h of exposure)	References
$CoCl_2$ (solution)	SHSY5Y SKNBE(2c)	Co^{2+}	NA	500 μM (containing 24.96×10^3 mg/ml of Co^{2+})	Cell viability (%) 23.43 ± 2.21 and 57.93 ± 3.47, respectively	Stenger et al. (2011)
SWCNT-3	A549	Fe^{2+}, Co^{2+}, Mo^{2+}	9.3, 4.8, 1.2	10 μg/ml (containing 0.93 μg/ml of Fe^{2+}, 0.48 μg/ml of Co^{2+} and 0.12 μg/ml of Mo^{2+})	Loss of cell viability (>20%)	Ge et al. (2012)
SWCNT	HUVEC	Co^{2+}	<3	50 μg/ml (containing <1.5 μg/ml of Co^{2+})	Loss of cell viability (>20%)	This study

Co^{2+} NIOSH REL: TWA 0.05 mg/m^3.

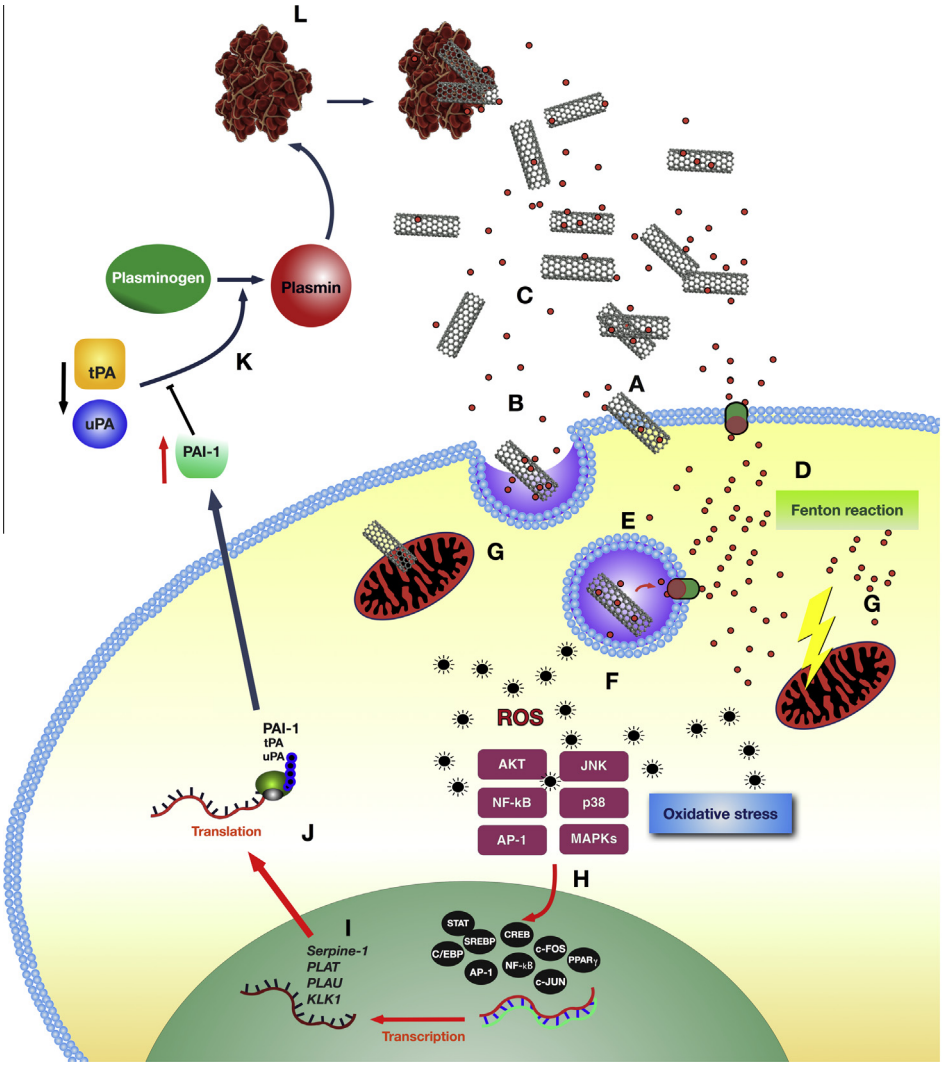

Fig. 9. Possible mechanism for cell damage, oxidative stress and alteration of SWCNTs on endothelial fibrinolysis-related genes and protein. (A) SWCNT-uptake to the cell by nanopenetration or passive transportation occurring when CNT crosses through the cell membrane; (B) SWCNT caveole-mediated endocytosis. (C) Extracellular SWCNT-metal leached. (D) Uptake of leached metals from SWCNT into the cell by transporters (i.e. metal transporter-1 for Co). (E) SWCNT-endocytosis and enhanced Co release in endosome and lysosome. (F). Fenton reaction by leached metals of SWCNTs (Co), increases in ROS production and then oxidative stress. (G) Chemical-mitochondrial damage by ROS and physical-mitochondrial damage by the SWCNTs structure. (H) Activation of some pathways by ROS and the consequent translocation of transcription factors. (I) Transcription of *serpine-1*-, *PLAT*-, *PLAU*- and *KLK1*-mRNA. (J) mRNA translation and differential synthesis of PAI-1, tPA and uPA, which are secreted to extracellular medium. (K) PAI-1, the most abundant and synthetized protein and the primary inhibitor of both tPA and uPA. A functional defect or an insufficient fibrinolysis response may lead to thrombosis with severe or fatal clinical consequences. (L) Thrombus may interact also with CNTs and increase their half-life and subsequently, form an occlusive arterial thrombi.

SWCNT-exposure and, in turn, by ROS to produce differential expressions of the genes evaluated. An illustration of the possible pathways affected by SWCNT-exposure is proposed in Fig. 9.

Therefore, the protein level analysis shown that PAI-1 had the highest levels, and its rise in expression was concentration-dependent in HUVEC treated with SWCNTs; however, tPA protein levels decreased, and uPA did not show significant changes. TNF-α, a

positive control, increased PAI-1 but did not increase tPA or uPA levels. Antioxidant co-treatment also diminished the protein levels, with the exception of PAI-1 at 5 μg/ml SWCNTs. The biological role of PAI-1 largely depends on its levels of expression, as well as its activity. PAI-1 is expressed in ECs and is regulated at the transcriptional, post-transcriptional and post-translational levels. PAI-1 gene expression is tightly regulated by a variety of cytokines and growth factors, including thrombin, endotoxin, dexamethasone, interleukin-1, transforming growth factor β (TGF-β) and TNF-α (van Hinsbergh et al., 1988; Nagamine, 2008; Kruithof, 1988). Hence, we used the latter as a positive control to induce endothelial activation, using the overexpression of PAI-1 as an indicator. Also of consideration is that high PAI-1 plasma concentrations have been shown to considerably shorten the tPA half-life in circulation and may lead to decreased fibrinolysis activity (Wiman, 2000). Although we used an *in vitro* system, we hypothesized that PAI-1 is secreted from HUVEC and increasing its level, which in turn, inhibits tPA and uPA proteins as indicated by the low levels observed here (Fig. 8).

5. Conclusion

The cytotoxicity of commercial and pristine SWCNTs in HUVEC may be related to the oxidative capacity of both CNTs and Co, the latter of which is an active ROS generator that acts through Fenton reactions. Our results suggest that SWCNTs were able to alter the expression of genes and proteins involved in fibrinolysis, which in turn may cause an endothelial dysfunction and develop a prothrombotic effect. These results may help to foresee possible pathologies caused by these novel materials. However, further mechanistic studies are needed to fully elucidate the effects of pristine-commercial SWCNTs on ECs to better understand and define the sequence of molecular events and regulatory mechanisms involved in SWCNT-induced endothelial dysfunction and fibrinolysis pathway alterations.

Authors' contributions

Y.R.Y. conceived the study, designed and performed experiments, analyzed data and wrote manuscript. R.L.M. and B.C. assisted in experimental work and read manuscript. D.B.U. and B.C.M. provided characterization images by TEM and STEM, read the manuscript and provided intellectual input. S.G.M. provided the umbilical cords. A.A. supervised work, read the manuscript and provided intellectual input throughout the study. All authors read and approved the manuscript.

Conflict of Interest

The authors declare that there are no conflicts of interest.

Transparency Document

The Transparency document associated with this article can be found in the online version.

Acknowledgements

This work was supported by the Grants: (1) Consejo Nacional de Ciencia y Tecnología (CONACyT), México, 162391 and (2) Instituto de Ciencia y Tecnología del Distrito Federal, México, 51/2012 to A.A.; Y.R.Y. received a CONACyT Grant: 203482. Authors gratefully acknowledged to Cinvestav and Hospital General de Ticomán SS-DF for collecting umbilical cords, as well as Biol. Pablo Gómez Islas and MSc. Victor Hugo Rosales for technical support in this study.

References

Albini, A., Mussi, V., Parodi, A., Ventura, A., Principi, E., Tegami, S., Rocchia, M., Franceschi, E., Sogno, I., Cammarota, R., Finzi, G., Sessa, F., Noonan, D.M., Valbusa, U., 2010. Interactions of single-wall carbon nanotubes with endothelial cells. Nanomed. Nanotechnol. Biol. Med. 6, 277–288.

Ali-Boucetta, H., Kostarelos, K., 2013. Pharmacology of carbon nanotubes: toxicokinetics, excretion and tissue accumulation. Adv. Drug Deliv. Rev. 65, 2111–2119.

Apopa, P.L., Qian, Y., Shao, R., Guo, N.L., Schwegler-Berry, D., Pacurari, M., Porter, D., Shi, X., Vallyathan, V., Castranova, V., Flynn, D.C., 2009. Iron oxide nanoparticles induce human microvascular endothelial cell permeability through reactive oxygen species production and microtubule remodeling. Particle Fibre Toxicol. 6, 1.

Azad, N., Iyer, A.K., Wang, L., Liu, Y., Lu, Y., Rojanasakul, Y., 2013. Reactive oxygen species-mediated p38 MAPK regulates carbon nanotube-induced fibrogenic and angiogenic responses. Nanotoxicology 7, 157–168.

Bachetti, T., Morbidelli, L., 2000. Endothelial cells in culture: a model for studying vascular functions. Pharmacol. Res.: Official J. Italian Pharmacol. Soc. 42, 9–19.

Banhart, F., 2009. Interactions between metals and carbon nanotubes: at the interface between old and new materials. Nanoscale 1, 201–213.

Baudin, B., Bruneel, A., Bosselut, N., Vaubourdolle, M., 2007. A protocol for isolation and culture of human umbilical vein endothelial cells. Nat. Protoc. 2, 481–485.

Bhoola, K.D., Figueroa, C.D., Worthy, K., 1992. Bioregulation of kinins: kallikreins, kininogens, and kininases. Pharmacol. Rev. 44, 1–80.

Bihari, P., Holzer, M., Praetner, M., Fent, J., Lerchenberger, M., Reichel, C.A., Rehberg, M., Lakatos, S., Krombach, F., 2010. Single-walled carbon nanotubes activate platelets and accelerate thrombus formation in the microcirculation. Toxicology 269, 148–154.

Binder, B.R., Christ, G., Gruber, F., Grubic, N., Hufnagl, P., Krebs, M., Mihaly, J., Prager, G.W., 2002. Plasminogen activator inhibitor 1: Physiological and pathophysiological roles. News Physiol. Sci.: Int. J. Physiol. Produced Jointly Int. Union Physiol. Sci. Am. Physiol. Soc. 17, 56–61.

Blechinger, J., Bauer, A.T., Torrano, A.A., Gorzelanny, C., Brauchle, C., Schneider, S.W., 2013. Uptake kinetics and nanotoxicity of silica nanoparticles are cell type dependent. Small 9 (3970–80), 3906.

Brown, N.J., Gainer, J.V., Murphey, L.J., Vaughan, D.E., 2000. Bradykinin stimulates tissue plasminogen activator release from human forearm vasculature through B(2) receptor-dependent, NO synthase-independent, and cyclooxygenase-independent pathway. Circulation 102, 2190–2196.

Bussy, C., Methven, L., Kostarelos, K., 2013. Hemotoxicity of carbon nanotubes. Adv. Drug Deliv. Rev. 65, 2127–2134.

Casey, A., Herzog, E., Lyng, F.M., Byrne, H.J., Chambers, G., Davoren, M., 2008. Single walled carbon nanotubes induce indirect cytotoxicity by medium depletion in A549 lung cells. Toxicol. Lett. 179, 78–84.

Charrier, J.G., Anastasio, C., 2012. On dithiothreitol (DTT) as a measure of oxidative potential for ambient particles: evidence for the importance of soluble transition metals. Atmos. Chem. Phys. 12, 11317–11350.

Cheng, W.W., Lin, Z.Q., Wei, B.F., Zeng, Q., Han, B., Wei, C.X., Fan, X.J., Hu, C.L., Liu, L.H., Huang, J.H., Yang, X., Xi, Z.G., 2011. Single-walled carbon nanotube induction of rat aortic endothelial cell apoptosis: reactive oxygen species are involved in the mitochondrial pathway. Int. J. Biochem. Cell Biol. 43, 564–572.

Dahm, M.M., Evans, D.E., Schubauer-Berigan, M.K., Birch, M.E., Fernback, J.E., 2012. Occupational exposure assessment in carbon nanotube and nanofiber primary and secondary manufacturers. Ann. Occup. Hyg. 56, 542–556.

Dahm, M.M., Evans, D.E., Schubauer-Berigan, M.K., Birch, M.E., Deddens, J.A., 2013. Occupational exposure assessment in carbon nanotube and nanofiber primary and secondary manufacturers: mobile direct-reading sampling. Ann. Occup. Hyg. 57, 328–344.

Ding, M., Shi, X., Lu, Y., Huang, C., Leonard, S., Roberts, J., Antonini, J., Castranova, V., Vallyathan, V., 2001. Induction of activator protein-1 through reactive oxygen species by crystalline silica in JB6 cells. J. Biol. Chem. 276, 9108–9114.

Ding, F., Larsson, P., Larsson, J.A., Ahuja, R., Duan, H., Rosen, A., Bolton, K., 2008. The importance of strong carbon-metal adhesion for catalytic nucleation of single-walled carbon nanotubes. Nano Lett. 8, 463–468.

Distefano, E., Eiguren-Fernandez, A., Delfino, R.J., Sioutas, C., Froines, J.R., Cho, A.K., 2009. Determination of metal-based hydroxyl radical generating capacity of ambient and diesel exhaust particles. Inhalation Toxicol. 21, 731–738.

Duan, J., Yu, Y., Li, Y., Yu, Y., Li, Y., Zhou, X., Huang, P., Sun, Z., 2013. Toxic effect of silica nanoparticles on endothelial cells through DNA damage response via Chk1-dependent G2/M checkpoint. PLoS ONE 8, e62087.

Erdely, A., Hulderman, T., Salmen, R., Liston, A., Zeidler-Erdely, P.C., Schwegler-Berry, D., Castranova, V., Koyama, S., Kim, Y.A., Endo, M., Simeonova, P.P., 2009. Cross-talk between lung and systemic circulation during carbon nanotube respiratory exposure. Potential biomarkers. Nano Lett. 9, 36–43.

Erdely, A., Dahm, M., Chen, B.T., Zeidler-Erdely, P.C., Fernback, J.E., Birch, M.E., Evans, D.E., Kashon, M.L., Deddens, J.A., Hulderman, T., Bilgesu, S.A., Battelli, L., Schwegler-Berry, D., Leonard, H.D., Mckinney, W., Frazer, D.G., Antonini, J.M., Porter, D.W., Castranova, V., Schubauer-Berigan, M.K., 2013. Carbon nanotube dosimetry: from workplace exposure assessment to inhalation toxicology. Particle Fibre Toxicol. 10, 53.

Firme 3rd, C.P., Bandaru, P.R., 2010. Toxicity issues in the application of carbon nanotubes to biological systems. Nanomed. Nanotechnol. Biol. Med. 6, 245–256.

Foldbjerg, R., Irving, E.S., Wang, J., Thorsen, K., Sutherland, D.S., Autrupa, H., Beer, C., 2014. The toxic effects of single-walled carbon nanotubes are linked to the phagocytic ability of cells. Toxicol. Res. UK 3, 228–241.
Ge, C.C., Li, Y., Yin, J.J., Liu, Y., Wang, L.M., Zhao, Y.L., Chen, C.Y., 2012. The contributions of metal impurities and tube structure to the toxicity of carbon nanotube materials. NPG Asia Mater. 4.
Geller, M.D., Ntziachristos, L., Mamakos, A., Samaras, Z., Schmitz, D.A., Froines, J.R., Sioutas, C., 2006. Physicochemical and redox characteristics of particulate matter (PM) emitted from gasoline and diesel passenger cars. Atmos. Environ. 40, 6988–7004.
Gojova, A., Guo, B., Kota, R.S., Rutledge, J.C., Kennedy, I.M., Barakat, A.I., 2007. Induction of inflammation in vascular endothelial cells by metal oxide nanoparticles: effect of particle composition. Environ. Health Perspect. 115, 403–409.
Guo, L., Von Dem Bussche, A., Buechner, M., Yan, A., Kane, A.B., Hurt, R.H., 2008. Adsorption of essential micronutrients by carbon nanotubes and the implications for nanotoxicity testing. Small 4, 721–727.
Guo, Y.Y., Zhang, J., Zheng, Y.F., Yang, J., Zhu, X.Q., 2011. Cytotoxic and genotoxic effects of multi-wall carbon nanotubes on human umbilical vein endothelial cells in vitro. Mutat. Res. 721, 184–191.
Gutierrez-Praena, D., Pichardo, S., Sanchez, E., Grilo, A., Camean, A.M., Jos, A., 2011. Influence of carboxylic acid functionalization on the cytotoxic effects induced by single wall carbon nanotubes on human endothelial cells (HUVEC). Toxicol. In Vitro: Int. J. Publ. Assoc. BIBRA 25, 1883–1888.
Han, J.H., Lee, E.J., Lee, J.H., So, K.P., Lee, Y.H., Bae, G.N., Lee, S.B., Ji, J.H., Cho, M.H., Yu, I.J., 2008. Monitoring multiwalled carbon nanotube exposure in carbon nanotube research facility. Inhalation Toxicol. 20, 741–749.
He, X., Wang, L., Szklarz, G., Bi, Y., Ma, Q., 2012. Resveratrol inhibits paraquat-induced oxidative stress and fibrogenic response by activating the nuclear factor erythroid 2-related factor 2 pathway. J. Pharmacol. Exp. Ther. 342, 81–90.
Heckel, K., Kiefmann, R., Dorger, M., Stoeckelhuber, M., Goetz, A.E., 2004. Colloidal gold particles as a new in vivo marker of early acute lung injury. Am. J. Physiol. Lung Cell. Mol. Physiol. 287, L867–L878.
Hedmer, M., Isaxon, C., Nilsson, P.T., Ludvigsson, L., Messing, M.E., Genberg, J., Skaug, V., Bohgard, M., Tinnerberg, H., Pagels, J.H., 2014. Exposure and emission measurements during production, purification, and functionalization of arc-discharge-produced multi-walled carbon nanotubes. Ann. Occup. Hyg. 58, 355–379.
Herzog, E., Casey, A., Lyng, F.M., Chambers, G., Byrne, H.J., Davoren, M., 2007. A new approach to the toxicity testing of carbon-based nanomaterials–the clonogenic assay. Toxicol. Lett. 174, 49–60.
Holt, B.D., Short, P.A., Rape, A.D., Wang, Y.L., Islam, M.F., Dahl, K.N., 2010. Carbon nanotubes reorganize actin structures in cells and ex vivo. ACS Nano 4, 4872–4878.
Hu, S., Polidori, A., Arhami, M., Shafer, M.M., Schauer, J.J., Cho, A., Sioutas, C., 2008. Redox activity and chemical speciation of size fractioned PM in the communities of the Los Angeles-Long Beach harbor. Atmos. Chem. Phys. 8, 6439–6451.
Iijima, S., 1991. Helical microtubules of graphitic carbon. Nature 354, 56–58.
Irigoyen, J.P., Munoz-Canoves, P., Montero, L., Koziczak, M., Nagamine, Y., 1999. The plasminogen activator system: biology and regulation. Cell. Mol. Life Sci.: CMLS 56, 104–132.
Jomova, K., Valko, M., 2011. Advances in metal-induced oxidative stress and human disease. Toxicology 283, 65–87.
Kalyanaraman, B., Darley-Usmar, V., Davies, K.J., Dennery, P.A., Forman, H.J., Grisham, M.B., Mann, G.E., Moore, K., Roberts 2nd, L.J., Ischiropoulos, H., 2012. Measuring reactive oxygen and nitrogen species with fluorescent probes: challenges and limitations. Free Radical Biol. Med. 52, 1–6.
Karin, M., Liu, Z., Zandi, E., 1997. AP-1 function and regulation. Curr. Opin. Cell Biol. 9, 240–246.
Kisin, E.R., Murray, A.R., Keane, M.J., Shi, X.C., Schwegler-Berry, D., Gorelik, O., Arepalli, S., Castranova, V., Wallace, W.E., Kagan, V.E., Shvedova, A.A., 2007. Single-walled carbon nanotubes: geno- and cytotoxic effects in lung fibroblast V79 cells. J. Toxicol. Environ. Health Part A 70, 2071–2079.
Kostarelos, K., Lacerda, L., Pastorin, G., Wu, W., Wieckowski, S., Luangsivilay, J., Godefroy, S., Pantarotto, D., Briand, J.P., Muller, S., Prato, M., Bianco, A., 2007. Cellular uptake of functionalized carbon nanotubes is independent of functional group and cell type. Nat. Nanotechnol. 2, 108–113.
Kruithof, E.K., 1988. Plasminogen activator inhibitors–a review. Enzyme 40, 113–121.
Kumagai, Y., Koide, S., Taguchi, K., Endo, A., Nakai, Y., Yoshikawa, T., Shimojo, N., 2002. Oxidation of proximal protein sulfhydryls by phenanthraquinone, a component of diesel exhaust particles. Chem. Res. Toxicol. 15, 483–489.
Lacerda, S.H., Semberova, J., Holada, K., Simakova, O., Hudson, S.D., Simak, J., 2011. Carbon nanotubes activate store-operated calcium entry in human blood platelets. ACS Nano 5, 5808–5813.
Lam, C.W., James, J.T., Mccluskey, R., Hunter, R.L., 2004. Pulmonary toxicity of single-wall carbon nanotubes in mice 7 and 90 days after intratracheal instillation. Toxicol. Sci.: Official J. Soc. Toxicol. 77, 126–134.
Lee, J.H., Lee, S.B., Bae, G.N., Jeon, K.S., Yoon, J.U., Ji, J.H., Sung, J.H., Lee, B.G., Lee, J.H., Yang, J.S., Kim, H.Y., Kang, C.S., Yu, I.J., 2010. Exposure assessment of carbon nanotube manufacturing workplaces. Inhalation Toxicol. 22, 369–381.
Leonard, S., Gannett, P.M., Rojanasakul, Y., Schwegler-Berry, D., Castranova, V., Vallyathan, V., Shi, X., 1998. Cobalt-mediated generation of reactive oxygen species and its possible mechanism. J. Inorg. Biochem. 70, 239–244.
Li, N., Sioutas, C., Cho, A., Schmitz, D., Misra, C., Sempf, J., Wang, M., Oberley, T., Froines, J., Nel, A., 2003. Ultrafine particulate pollutants induce oxidative stress and mitochondrial damage. Environ. Health Perspect. 111, 455–460.
Marangon, I., Boggetto, N., Menard-Moyon, C., Venturelli, E., Beoutis, M.L., Pechoux, C., Luciani, N., Wilhelm, C., Bianco, A., Gazeau, F., 2012. Intercellular carbon nanotube translocation assessed by flow cytometry imaging. Nano Lett. 12, 4830–4837.
Maynard, A.D., Baron, P.A., Foley, M., Shvedova, A.A., Kisin, E.R., Castranova, V., 2004. Exposure to carbon nanotube material: aerosol release during the handling of unrefined single-walled carbon nanotube material. J. Toxicol. Environ. Health Part A 67, 87–107.
Meng, J., Cheng, X., Liu, J., Zhang, W., Li, X., Kong, H., Xu, H., 2012. Effects of long and short carboxylated or aminated multiwalled carbon nanotubes on blood coagulation. PLoS ONE 7, e38995.
Methner, M., Beaucham, C., Crawford, C., Hodson, L., Geraci, C., 2012. Field application of the nanoparticle emission assessment technique (NEAT): task-based air monitoring during the processing of engineered nanomaterials (ENM) at four facilities. J. Occup. Environ. Hyg. 9, 543–555.
Monteiro-Riviere, N.A., Nemanich, R.J., Inman, A.O., Wang, Y.Y., Riviere, J.E., 2005. Multi-walled carbon nanotube interactions with human epidermal keratinocytes. Toxicol. Lett. 155, 377–384.
Montiel-Davalos, A., Ventura-Gallegos, J.L., Alfaro-Moreno, E., Soria-Castro, E., Garcia-Latorre, E., Cabanas-Moreno, J.G., Del Pilar Ramos-Godinez, M., Lopez-Marure, R., 2012. TiO(2) nanoparticles induce dysfunction and activation of human endothelial cells. Chem. Res. Toxicol. 25, 920–930.
Murray, A.R., Kisin, E., Leonard, S.S., Young, S.H., Kommineni, C., Kagan, V.E., Castranova, V., Shvedova, A.A., 2009. Oxidative stress and inflammatory response in dermal toxicity of single-walled carbon nanotubes. Toxicology 257, 161–171.
Nagamine, Y., 2008. Transcriptional regulation of the plasminogen activator inhibitor type 1–with an emphasis on negative regulation. Thromb. Haemost. 100, 1007–1013.
Nemmar, A., Hoet, P.H., Vanquickenborne, B., Dinsdale, D., Thomeer, M., Hoylaerts, M.F., Vanbilloen, H., Mortelmans, L., Nemery, B., 2002. Passage of inhaled particles into the blood circulation in humans. Circulation 105, 411–414.
Nemmar, A., Hoylaerts, M.F., Hoet, P.H., Nemery, B., 2004. Possible mechanisms of the cardiovascular effects of inhaled particles: systemic translocation and prothrombotic effects. Toxicol. Lett. 149, 243–253.
NIOSH, 2013. Current Intelligence Bulletin 65: Occupational Exposure to Carbon Nanotubes and Nanofibers. Publication Number: 2013–145.
Ntziachristos, L., Froines, J.R., Cho, A.K., Sioutas, C., 2007. Relationship between redox activity and chemical speciation of size-fractionated particulate matter. Particle Fibre Toxicol. 4, 5.
Pacurari, M., Yin, X.J., Zhao, J., Ding, M., Leonard, S.S., Schwegler-Berry, D., Ducatman, B.S., Sbarra, D., Hoover, M.D., Castranova, V., Vallyathan, V., 2008. Raw single-wall carbon nanotubes induce oxidative stress and activate MAPKs, AP-1, NF-kappaB, and Akt in normal and malignant human mesothelial cells. Environ. Health Perspect. 116, 1211–1217.
Pacurari, M., Qian, Y., Fu, W., Schwegler-Berry, D., Ding, M., Castranova, V., Guo, N.L., 2012. Cell permeability, migration, and reactive oxygen species induced by multiwalled carbon nanotubes in human microvascular endothelial cells. J. Toxicol. Environ. Health Part A 75, 129–147.
Popov, V.N., 2004. Carbon nanotubes: properties and application. Mater. Sci. Eng. R: Rep. 43, 61–102.
Porter, A.E., Gass, M., Muller, K., Skepper, J.N., Midgley, P.A., Welland, M., 2007. Direct imaging of single-walled carbon nanotubes in cells. Nat. Nanotechnol. 2, 713–717.
Porter, D.W., Hubbs, A.F., Mercer, R.R., Wu, N., Wolfarth, M.G., Sriram, K., Leonard, S., Battelli, L., Schwegler-Berry, D., Friend, S., Andrew, M., Chen, B.T., Tsuruoka, S., Endo, M., Castranova, V., 2010. Mouse pulmonary dose- and time course-responses induced by exposure to multi-walled carbon nanotubes. Toxicology 269, 136–147.
Pulskamp, K., Diabate, S., Krug, H.F., 2007. Carbon nanotubes show no sign of acute toxicity but induce intracellular reactive oxygen species in dependence on contaminants. Toxicol. Lett. 168, 58–74.
Radomski, A., Jurasz, P., Alonso-Escolano, D., Drews, M., Morandi, M., Malinski, T., Radomski, M.W., 2005. Nanoparticle-induced platelet aggregation and vascular thrombosis. Br. J. Pharmacol. 146, 882–893.
Rein-Smith, C.M., Church, F.C., 2014. Emerging pathophysiological roles for fibrinolysis. Curr. Opin. Hematol. 21, 438–444.
Rodriguez-Yanez, Y., Munoz, B., Albores, A., 2013. Mechanisms of toxicity by carbon nanotubes. Toxicol. Mech. Methods 23, 178–195.
Sargent, L.M., Shvedova, A.A., Hubbs, A.F., Salisbury, J.L., Benkovic, S.A., Kashon, M.L., Lowry, D.T., Murray, A.R., Kisin, E.R., Friend, S., Mckinstry, K.T., Battelli, L., Reynolds, S.H., 2009. Induction of aneuploidy by single-walled carbon nanotubes. Environ. Mol. Mutagen. 50, 708–717.
Sato, Y., Yokoyama, A., Shibata, K., Akimoto, Y., Ogino, S., Nodasaka, Y., Kohgo, T., Tamura, K., Akasaka, T., Uo, M., Motomiya, K., Jeyadevan, B., Ishiguro, M., Hatakeyama, R., Watari, F., Tohji, K., 2005. Influence of length on cytotoxicity of multi-walled carbon nanotubes against human acute monocytic leukemia cell line THP-I in vitro and subcutaneous tissue of rats in vivo. Mol. BioSyst. 1, 176–182.
Semberova, J., De Paoli Lacerda, S.H., Simakova, O., Holada, K., Gelderman, M.P., Simak, J., 2009. Carbon nanotubes activate blood platelets by inducing extracellular Ca^{2+} influx sensitive to calcium entry inhibitors. Nano Lett. 9, 3312–3317.

Shen, H., Anastasio, C., 2012. A comparison of hydroxyl radical and hydrogen peroxide generation in ambient particle extracts and laboratory metal solutions. Atmos. Environ. 46, 665–668.
Shvedova, A.A., Castranova, V., Kisin, E.R., Schwegler-Berry, D., Murray, A.R., Gandelsman, V.Z., Maynard, A., Baron, P., 2003. Exposure to carbon nanotube material: assessment of nanotube cytotoxicity using human keratinocyte cells. J. Toxicol. Environ. Health A 66, 1909–1926.
Shvedova, A.A., Kisin, E.R., Mercer, R., Murray, A.R., Johnson, V.J., Potapovich, A.I., Tyurina, Y.Y., Gorelik, O., Arepalli, S., Schwegler-Berry, D., Hubbs, A.F., Antonini, J., Evans, D.E., Ku, B.K., Ramsey, D., Maynard, A., Kagan, V.E., Castranova, V., Baron, P., 2005. Unusual inflammatory and fibrogenic pulmonary responses to single-walled carbon nanotubes in mice. Am. J. Physiol.. Lung Cell. Mol. Physiol. 289, L698–L708.
Shvedova, A.A., Kisin, E., Murray, A.R., Johnson, V.J., Gorelik, O., Arepalli, S., Hubbs, A.F., Mercer, R.R., Keohavong, P., Sussman, N., Jin, J., Yin, J., Stone, S., Chen, B.T., Deye, G., Maynard, A., Castranova, V., Baron, P.A., Kagan, V.E., 2008. Inhalation vs. aspiration of single-walled carbon nanotubes in C57BL/6 mice: inflammation, fibrosis, oxidative stress, and mutagenesis. Am. J. Physiol. Lung Cell. Mol. Physiol. 295, L552–L565.
Simon-Deckers, A., Gouget, B., Mayne-L'hermite, M., Herlin-Boime, N., Reynaud, C., Carriere, M., 2008. In vitro investigation of oxide nanoparticle and carbon nanotube toxicity and intracellular accumulation in A549 human pneumocytes. Toxicology 253, 137–146.
Snyder-Talkington, B.N., Schwegler-Berry, D., Castranova, V., Qian, Y., Guo, N.L., 2013. Multi-walled carbon nanotubes induce human microvascular endothelial cellular effects in an alveolar-capillary co-culture with small airway epithelial cells. Particle Fibre Toxicol. 10, 35.
Stenger, C., Naves, T., Verdier, M., Ratinaud, M.H., 2011. The cell death response to the ROS inducer, cobalt chloride, in neuroblastoma cell lines according to p53 status. Int. J. Oncol. 39, 601–609.
Tian, F., Cui, D., Schwarz, H., Estrada, G.G., Kobayashi, H., 2006. Cytotoxicity of single-wall carbon nanotubes on human fibroblasts. Toxicol. In Vitro: Int. J. Publ. Assoc. BIBRA 20, 1202–1212.
Van Hinsbergh, V.W., Kooistra, T., Van Den Berg, E.A., Princen, H.M., Fiers, W., Emeis, J.J., 1988. Tumor necrosis factor increases the production of plasminogen activator inhibitor in human endothelial cells in vitro and in rats in vivo. Blood 72, 1467–1473.
Vesterdal, L.K., Mikkelsen, L., Folkmann, J.K., Sheykhzade, M., Cao, Y., Roursgaard, M., Loft, S., Moller, P., 2012. Carbon black nanoparticles and vascular dysfunction in cultured endothelial cells and artery segments. Toxicol. Lett. 214, 19–26.
Vidanapathirana, A.K., Lai, X., Hilderbrand, S.C., Pitzer, J.E., Podila, R., Sumner, S.J., Fennell, T.R., Wingard, C.J., Witzmann, F.A., Brown, J.M., 2012. Multi-walled carbon nanotube directed gene and protein expression in cultured human aortic endothelial cells is influenced by suspension medium. Toxicology 302, 114–122.
Vidrio, E., Phuah, C.H., Dillner, A.M., Anastasio, C., 2009. Generation of hydroxyl radicals from ambient fine particles in a surrogate lung fluid solution. Environ. Sci. Technol. 43, 922–927.
Walker, V.G., Li, Z., Hulderman, T., Schwegler-Berry, D., Kashon, M.L., Simeonova, P.P., 2009. Potential in vitro effects of carbon nanotubes on human aortic endothelial cells. Toxicol. Appl. Pharmacol. 236, 319–328.
Wang, X., Xia, T., Ntim, S.A., Ji, Z., George, S., Meng, H., Zhang, H., Castranova, V., Mitra, S., Nel, A.E., 2010a. Quantitative techniques for assessing and controlling the dispersion and biological effects of multiwalled carbon nanotubes in mammalian tissue culture cells. ACS Nano 4, 7241–7252.
Wang, Y., Arellanes, C., Curtis, D.B., Paulson, S.E., 2010b. Probing the source of hydrogen peroxide associated with coarse mode aerosol particles in southern California. Environ. Sci. Technol. 44, 4070–4075.
Warheit, D.B., 2009. Long-term inhalation toxicity studies with multiwalled carbon nanotubes: closing the gaps or initiating the debate? Toxicol. Sci.: Official J. Soc. Toxicol. 112, 273–275.
Wick, P., Manser, P., Limbach, L.K., Dettlaff-Weglikowska, U., Krumeich, F., Roth, S., Stark, W.J., Bruinink, A., 2007. The degree and kind of agglomeration affect carbon nanotube cytotoxicity. Toxicol. Lett. 168, 121–131.
Wiman, B., 2000. The fibrinolytic enzyme system. Basic principles and links to venous and arterial thrombosis. Hematol./Oncol. Clin. North Am. 14, 325–338, vii.
Worle-Knirsch, J.M., Pulskamp, K., Krug, H.F., 2006. Oops they did it again! Carbon nanotubes hoax scientists in viability assays. Nano Lett. 6, 1261–1268.
Wu, X., Tan, Y., Mao, H., Zhang, M., 2010. Toxic effects of iron oxide nanoparticles on human umbilical vein endothelial cells. Int. J. Nanomed. 5, 385–399.
Zhiqing, L., Zhuge, X., Fuhuan, C., Danfeng, Y., Huashan, Z., Bencheng, L., Wei, Z., Huanliang, L., Xin, S., 2010. ICAM-1 and VCAM-1 expression in rat aortic endothelial cells after single-walled carbon nanotube exposure. J. Nanosci. Nanotechnol. 10, 8562–8574.
Zhu, L., Chang, D.W., Dai, L., Hong, Y., 2007. DNA damage induced by multiwalled carbon nanotubes in mouse embryonic stem cells. Nano Lett. 7, 3592–3597.
Zhu, M.T., Wang, B., Wang, Y., Yuan, L., Wang, H.J., Wang, M., Ouyang, H., Chai, Z.F., Feng, W.Y., Zhao, Y.L., 2011. Endothelial dysfunction and inflammation induced by iron oxide nanoparticle exposure: risk factors for early atherosclerosis. Toxicol. Lett. 203, 162–171.